Redox Biology 2 (2014) 755–763

Contents lists available at ScienceDirect

Redox Biology

journal homepage: www.elsevier.com/locate/redox

Research Paper

Identification of a negative feedback loop in biological oxidant formation fegulated by 4-hydroxy-2-(*E*)-nonenal

Tonibelle N. Gatbonton-Schwager[a], Sushabhan Sadhukhan[b], Guo-Fang Zhang[c], John J. Letterio[a,d], Gregory P. Tochtrop[a,b,*]

[a]Department of Pharmacology, Case Western Reserve University, 10900 Euclid Avenue, Cleveland, OH 44106, USA
[b]Department of Chemistry, Case Western Reserve University, 10900 Euclid Avenue, Cleveland, OH 44106, USA
[c]Department of Nutrition, Case Western Reserve University, 10900 Euclid Avenue, Cleveland, OH 44106, USA
[d]Department of Pediatrics, Case Western Reserve University, 10900 Euclid Avenue, Cleveland, OH 44106, USA

ARTICLE INFO

Article history:
Received 4 April 2014
Received in revised form 21 April 2014
Accepted 22 April 2014

Keywords:
lipid peroxidation
4-HNE
iNOS
nitric oxide
Nrf2

ABSTRACT

4-Hydroxy-2-(*E*)-nonenal (4-HNE) is one of the major lipid peroxidation product formed during oxidative stress. At high concentrations, 4-HNE is cytotoxic and exerts deleterious effects that are often associated with the pathology of oxidative stress-driven disease. Alternatively, at low concentrations it functions as a signaling molecule that can activate protective pathways including the antioxidant Nrf2-Keap1 pathway. Although these biphasic signaling properties have been enumerated in many diseases and pathways, it has yet to be addressed whether 4-HNE has the capacity to modulate oxidative stress-driven lipid peroxidation. Here we report an auto-regulatory mechanism of 4-HNE via modulation of the biological oxidant nitric oxide (NO). Utilizing LPS-activated macrophages to induce biological oxidant production, we demonstrate that 4-HNE modulates NO levels via inhibition of iNOS expression. We illustrate a proposed model of control of NO formation whereby at low concentrations of 4-HNE a negative feedback loop maintains a constant level of NO production with an observed inflection at approximately 1 μM, while at higher 4-HNE concentrations positive feedback is observed. Further, we demonstrate that this negative feedback loop of NO production control is dependent on the Nrf2-Keap1 signaling pathway. Taken together, the careful regulation of NO production by 4-HNE argues for a more fundamental role of this lipid peroxidation product in normal physiology.

Introduction

Polyunsaturated fatty acids (PUFAs) may undergo both enzymatic and non-enzymatic lipid peroxidation leading to unsaturated lipid hydroperoxides (LOOHs). The aforementioned enzymatic processes are mediated by members of the lipoxygenase family and lead to the formation of a family of physiologic mediators of inflammation, such as leukotrienes and prostaglandins [3,11,20,30]. The latter represents an altogether different and much less understood process whereby PUFAs, under conditions of oxidative stress, can spontaneously form peroxides at the allylic (or doubly allylic) positions initiated by a free radical hydrogen abstraction of a number of physiologic lipids [34,35]. These lipid peroxides can subsequently undergo a variety of secondary reactions, some leading to stable oxygenated and polyoxygenated acyl chains, while others lead to chain cleavage and products containing either a methyl or carboxy terminus. 4-Hydroxy-2-(*E*)-nonenal (4-HNE) is the most abundant of the known lipid peroxidation (LPO) products and is an established marker of oxidative stress. The pathogenicity of this reactive aldehyde has been rationalized through the formation of adducts with nucleophilic sites on proteins and DNA [27,38] and has become accepted as a modulator of multiple disease states, including Alzheimer's disease [2,7], atherosclerosis [5,37,42], and cancer [29]. However, the recent view regarding 4-HNE has evolved to appreciate the complex physiology and signaling aspects of this molecule [14,28,32].

To better understand these signaling properties and to explore whether 4-HNE could impact the formation of biological oxidants, we initiated a series of experiments examining the relationship between 4-HNE concentrations and the ability of activated cultured macrophages to produce nitric oxide (NO). Our rationale behind these experiments was based on previous work showing that 4-HNE activates the antioxidant Nrf2-Keap1 signaling pathway due to its electrophilic nature [8,19,21]. This coupled with our own work [16] as

* Corresponding author at: Department of Pharmacology, Case Western Reserve University, 10900 Euclid Avenue, Cleveland, OH 44106, USA.
E-mail address: tochtrop@case.edu (G.P. Tochtrop).

http://dx.doi.org/10.1016/j.redox.2014.04.009

well as others [12,23] showing that molecules which activate Nrf2 transcription also perturb inducible nitric oxide synthase (iNOS) expression and thus production of NO set the basis for the experiments described herein.

Experimental Section

Materials

The leukemic mouse macrophage cells (RAW 264.7) were obtained as a gift from Dr. Michael Sporn (Dartmouth College, NH). DMEM media was purchased from GIBCO (Grand Island, NY) and supplemented with low endotoxin FBS (< 0.06 EU) from Thermo Scientific (Logan, UT). DMSO, lipopolysaccharide (LPS) from *Escherichia coli*, and non-enzymatic cell detachment solution were purchased from Sigma (St. Louis, MO). Penicillin/streptomycin, Griess Reagent Kit (Griess assay), RIPA Buffer, 0.2 μm PVDF membrane, Novex® 4–20% Tris–Glycine gels, running and transfer buffers, PureLink™ RNA Mini Kit, Superscript® III Reverse Transcriptase and TaqMan® Fast Universal PCR Master Mix were all purchased from Invitrogen (Grand Island, NY). All the primary antibodies were purchased from Santa Cruz Biotechnology (Santa Cruz, CA) and secondary antibodies from Southern Biotech (Birmingham, AL). Recombinant mouse M-CSF was purchased from PeproTech (Rocky Hill, NJ). Protease cocktail inhibitor tablet was purchased from Roche (Indianapolis, IN) and PBS purchased from Cellgro by Mediatech, Inc. (Manassas, VA). The ECL plus was purchased from Amersham (Buckinghamshire, UK) and the autoradiography film was from MidSci (St. Louis, MO). The MTT cell proliferation assay kit was purchased from ATCC (Manassas, VA). The iNOS probe was purchased from Applied Biosystems (Carlsbad, CA), and the 18s rRNA probe was purchased from IDT (Coralville, IA). The iNOS activity kit and the murine recombinant iNOS were purchased from Cayman Chemicals (Ann Arbor, MI) and the [^{3}H] arginine monohydrochloride from PerkinElmer (Waltham, MA).

General methods for synthesis

Unless otherwise stated, the solvents and reagents were commercially available analytical grade quality and used without further purification. Flash chromatography was performed on silica gel (230–400 mesh) purchased from Dynamics Adsorbents (Atlanta, GA). TLC was done on Hard Layer, Organic Binder TLC-plates with a fluorescent indicator and visualized by UV light (254 nm) purchased from Dynamics Adsorbents (Atlanta, GA). ^{1}H and ^{13}C NMR spectra were recorded on a Varian Inova spectrometer (at the Department of Chemistry, Case Western Reserve University) operating at 400 MHz and 100 MHz for the ^{1}H and ^{13}C NMR spectra, respectively. The internal references were TMS (δ 0.00) and $CDCl_3$ (δ 77.2) for ^{1}H and ^{13}C spectra, respectively. NMR data are presented in the following order: chemical shift, peak multiplicity (b is the broad, s is the singlet, d is the doublet, t is the triplet, q is the quartet, m is the multiplet, dd is the doublet of doublet), coupling constant, and proton number.

Fumaraldehyde dimethylacetal (FDMA, 2)

Fumaraldehyde dimethylacetal, (FDMA, **2**) was obtained by partial acid hydrolysis of fumaraldehyde bis(dimethylacetal), (FbisDMA, **1**). Amberlyst-15 catalyst in acid form (0.06 g) was added to the FbisDMA **1** (0.2 g, 1.135 mmol) in acetone (6 mL) and water (0.08 mL) under magnetic stirring at room temperature. Stirring was continued for 10 min (longer time resulted in the hydrolysis of the second acetal group), then the reaction mixture was filtered through a bed of anhydrous sodium carbonate and sodium sulfate 1:1 (w:w) followed by the solvent evaporation *in vacuo* to obtain FDMA [2] (0.14 g, 1.076 mmol, 95% yield). NMR data were in accord with the literature [10].

4-Hydroxy-2-(E)-pentenal (4-HPE, 3)

A solution of aldehyde, FDMA [2] (0.14 g, 1.076 mmol) in dry THF (6 mL) was cooled to −78 °C, and 0.8 mL of MeLi (1.6 M solution in Et_2O, 1.28 mmol) was added slowly. The solution was stirred for 30 min followed by work-up with saturated solution of NH_4Cl at −78 °C. The reaction mixture was then extracted with Et_2O (3 × 10 mL), the combined organic layers were dried over Na_2SO_4, and the solvent was removed *in vacuo* to obtain the crude product. The latter was then hydrolyzed with Amberlyst-15 as described for FDMA [2] to afford the crude 4-hydroxy-2-(*E*)-pentenal (4-HPE, **3**), which was then purified by column chromatography over silica (hexane, 30% ethyl acetate) to give 4-HPE [3] (0.083 g, 0.829 mmol, 77%). ^{1}H NMR (400 MHz, $CDCl_3$): 1.39 (d, 3H, J = 6.8 Hz), 4.61 (m, 1H), 6.29 (ddd, 1H, J = 15.6, 7.6, 1.6 Hz), 6.84 (dd, 1H, J = 15.6, 4.8 Hz), 9.57 (d, 1H, J = 7.6 Hz); ^{13}C NMR (100 MHz, $CDCl_3$): 22.7, 67.3, 130.2, 160.1, 193.9. EI-HRMS (positive mode): m/z Calcd. for $C_5H_9O_2$ [MH^+] 101.0602, found 101.0602.

General method for 4-haydroxy-2-(E)-alkenals (3a–3g)

4-Hydroxy-2-(*E*)-alkenals, **3a–3g** were synthesized using the Gardner method (see Fig. 2A) [15]. To a stirring solution of 3-alkenol, **4a–4g** (1 mmol) in 4 mL CH_2Cl_2 was added a 1.5 M excess of 70% *m*-chloroperoxybenzoic acid (0.37 g). The solution was stirred at room temperature for 1.5 h after which 4 mL of 10% $NaHCO_3$ was added with vigorous stirring for 45 min. The reaction mixture was then extracted with CH_2Cl_2 (3 × 15 mL), the combined organic layers were dried over Na_2SO_4, and the solvent was removed *in vacuo* to obtain the crude product which was redissolved in 5 mL of CH_2Cl_2 and 6.6 mL of Dess–Martin periodinane (0.3 M solution in CH_2Cl_2, 2 mmol) was added. The mixture was stirred for 2 h at room temperature and then 15 mL of Et_2O and 8 mL of 1.3 M NaOH Was added into that and vigorously stirred for 1 min. The aqueous NaOH layer was removed, and an additional 10 mL of 1.3 M NaOH were added with vigorous stirring for 15 min. The aqueous layer was removed and the organic phase was washed with brine solution. The organic layer was dried over Na_2SO_4, and the solvent was removed *in vacuo* to obtain the crude 4-hydroxy-2-(*E*)-alkenal, which was then purified by column chromatography over silica (hexane, 30–40% ethyl acetate) to give pure 4-hydroxy-2-(*E*)-alkenal, **3a–3g**.

4-Hydroxy-2-(E)-hexenal (4-HHE, 3a)

Overall yield: 42.1% (0.048 g, 0.421 mmol); ^{1}H NMR (400 MHz, $CDCl_3$): 0.98 (t, 3H, J = 7.6 Hz), 1.57–1.74 (m, 2H), 4.36 (m, 1H), 6.29 (ddd, 1H, J = 15.6, 8.0, 1.6 Hz), 6.82 (dd, 1H, J = 15.6, 4.8 Hz), 9.55 (d, 1H, J = 8.0 Hz); ^{13}C NMR (100 MHz, $CDCl_3$): 9.6, 29.5, 72.3, 130.9, 159.3, 193.9. EI-HRMS (positive mode): m/z Calcd. for $C_6H_{11}O_2$ [MH^+] 115.0756, found 115.0756.

4-Hydroxy-2-(E)-heptenal (4-HHE, 3b)

Overall yield: 40% (0.051 g, 0.40 mmol); ^{1}H NMR (400 MHz, $CDCl_3$): 0.92 (t, 3H, J = 7.6 Hz), 1.32–1.61 (m, 4H), 4.41 (m, 1H), 6.27 (ddd, 1H, J = 15.6, 8.0, 1.6 Hz), 6.82 (dd, 1H, J = 15.6, 4.8 Hz), 9.52 (d, 1H, J = 8.0 Hz); ^{13}C NMR (100 MHz, $CDCl_3$): 14.1, 18.7, 38.6, 70.9, 130.6, 160.1, 194.2. EI-HRMS (positive mode): m/z Calcd. for $C_7H_{13}O_2$ [MH^+] 129.0915, found 129.0919.

4-Hydroxy-2-(E)-octenal (4-HOE, 3c)

Overall yield: 43% (0.061 g, 0.43 mmol); ^{1}H NMR (400 MHz, $CDCl_3$): 0.89 (t, 3H, J = 7.6 Hz), 1.28–1.66 (m, 6H), 4.40 (m, 1H), 6.28 (ddd, 1H, J = 15.6, 8.0, 1.6 Hz), 6.82 (dd, 1H, J = 15.6, 4.8 Hz), 9.53 (d, 1H, J = 8.0 Hz); ^{13}C NMR (100 MHz, $CDCl_3$): 14.1, 22.7, 27.5, 36.3, 71.2, 130.7, 159.9, 194.1. EI-HRMS (positive mode): m/z Calcd. for $C_8H_{15}O_2$ [MH^+] 143.1072, found 143.1078.

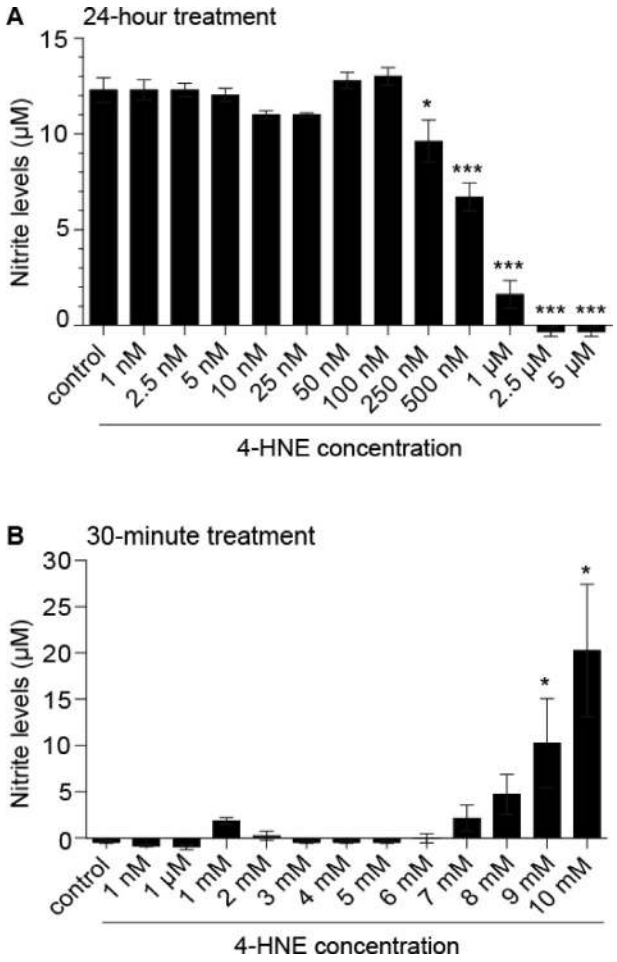

Fig. 1. Nitrite levels in 4-HNE treated LPS-activated RAW 264.7 cells. Nitrite levels were measured via Griess assay in cells simultaneously activated with 10 ng/mL LPS and treated with varying concentrations of 4-HNE for (A) 24 h and (B) 30 min. 0.25% DMSO was used as control. Experiments were performed at least 3 times and error bars represent standard error of mean. $^{*}P < 0.05$; $^{***}P < 0.001$.

4-Hydroxy-2-(E)-nonenal (4-HNE, 3d)

Overall yield: 46% (0.072 g, 0.46 mmol); ^{1}H NMR (400 MHz, $CDCl_3$): 0.94 (t, 3H, $J = 7.6$ Hz), 1.29–1.68 (m, 8H), 4.41 (m, 1H), 6.27 (ddd, 1H, $J = 15.6$, 8.0, 1.6 Hz), 6.82 (dd, 1H, $J = 15.6$, 4.8 Hz), 9.51 (d, 1H, $J = 8.0$ Hz); ^{13}C NMR (100 MHz, $CDCl_3$): 14.2, 22.7, 25.1, 31.8, 36.6, 71.3, 130.7, 159.6, 194.0. EI-HRMS (positive mode): m/z Calcd. for $C_9H_{17}O_2$ [MH^+] 157.1228, found 157.1231.

4-Hydroxy-2-(E)-decenal (4-HDE, 3e)

Overall yield: 39% (0.066 g, 0.39 mmol); ^{1}H NMR (400 MHz, $CDCl_3$): 0.90 (t, 3H, $J = 7.6$ Hz), 1.29–1.65 (m, 10H), 4.44 (m, 1H), 6.31 (ddd, 1H, $J = 15.6$, 8.0, 1.6 Hz), 6.84 (dd, 1H, $J = 15.6$, 4.8 Hz), 9.57 (d, 1H, $J = 8.0$ Hz); ^{13}C NMR (100 MHz, $CDCl_3$): 14.2, 22.7, 25.3, 29.2, 31.8, 36.6, 71.3, 130.7, 159.5, 194.0. EI-HRMS (positive mode): m/z Calcd. for $C_{10}H_{19}O_2$ [MH^+] 171.1385, found 171.1388.

4-Hydroxy-2-(E)-undecenal (4-HUE, 3f)

Overall yield: 41% (0.076 g, 0.41 mmol); ^{1}H NMR (400 MHz, $CDCl_3$): 0.90 (t, 3H, $J = 7.6$ Hz), 1.28–1.67 (m, 12H), 4.43 (m, 1H), 6.32 (ddd, 1H, $J = 15.6$, 8.0, 1.6 Hz), 6.83 (dd, 1H, $J = 15.6$, 4.8 Hz), 9.58 (d, 1H, $J = 8.0$ Hz); ^{13}C NMR (100 MHz, $CDCl_3$): 14.2, 22.8, 25.4, 29.3, 29.5, 31.9, 36.7, 71.3, 130.8, 159.4, 193.9. EI-HRMS (positive mode): m/z Calcd. for $C_{11}H_{21}O_2$ [MH^+] 181.1541, found 181.1541.

4-Hydroxy-2-(E)-dodecenal (4-HDoE, 3g)

Overall yield: 44% (0.087 g, 0.44 mmol); ^{1}H NMR (400 MHz, $CDCl_3$): 0.92 (t, 3H, $J = 7.6$ Hz), 1.25–1.66 (m, 14H), 4.44 (m, 1H), 6.31 (ddd, 1H, $J = 15.6$, 8.0, 1.6 Hz), 6.84 (dd, 1H, $J = 15.6$, 4.8 Hz), 9.58 (d, 1H, $J = 8.0$ Hz); ^{13}C NMR (100 MHz, $CDCl_3$): 14.3, 22.8, 25.4, 29.4, 29.6, 29.7, 32.0, 36.7, 71.3, 130.8, 159.3, 193.8. EI-HRMS (positive mode): m/z Calcd. for $C_{12}H_{23}O_2$ [MH^+] 199.1698, found 199.1702.

3-Alken-1-ol (4a-4g)

4a–4d were purchased from TCI America. The *cis*-3-decen-1-ol (**4e**) was obtained by catalytic semi hydrogenation (1 atm) of a solution of 3-decyn-1-ol. 3-Decyn-1-ol (1 g, 6.483 mmol) was dissolved in dry Et_2O (25 mL) in a small round bottom flask. Lindlar catalyst (50 mg, Pd on $CaCO_3$) and 1 g of quinoline were added and hydrogen was supplied from balloons. After completion of the reaction (confirmed by NMR) the mixture was filtered to remove the catalyst and the solvent was removed on a rotary evaporator. Dichloromethane was added to the residue and washed with 1M acetic acid, brine, and water, and dried with Na_2SO_4. The crude was then purified by column chromatography over silica (dichloromethane, 1% methanol) to afford *cis*-3-decen-1-ol, **4e** (0.932 g, 5.964 mmol, 92%). ^{1}H NMR (400 MHz, $CDCl_3$): 0.89 (t, 3*H*, $J = 6.8$ Hz), 1.23–1.55 (m, 8 H), 2.08 (td, 2*H*, $J = 6.8$, 6.6 Hz), 2.37 (td, 2*H*, $J = 6.6$, 6.4 Hz), 3.63 (td, 2*H*, $J = 5.8$, 5.6 Hz), 5.31–5.39 (m, 1 H), 5.51–5.63 (m, 1 H); ^{13}C NMR (100 MHz, $CDCl_3$): 14.1, 22.6, 27.3, 29.0, 29.6, 30.8, 31.8, 62.4, 124.8, 133.8.

Trans-3-undecen-1-ol

(**4f**) and trans-3-dodecen-1-ol (**4 g**) were synthesized using a Knoevenagel condensation of nonanal or decanal and malonic acid [31] followed by $LiAlH_4$ reduction. Malonic acid (2.03 g, 19.5 mmol) was dissolved in triethylamine (2.97 g, 29.27 mmol) in a 2-neck round-bottom flask fitted with a magnetic stirring bar and a reflux condenser. Nonanal (2.77 g, 19.5 mmol) was added very slowly under inert atmosphere at room temperature. The reaction mixture was then heated to 80 °C and maintained at this temperature for 3 h. The product was then acidified with 1 M HCl and extracted with Et_2O. Organic layers were thoroughly washed with brine and water and dried over Na_2SO_4. Solvent was removed *in vacuo* to obtain trans-3-undecenoic acid (2.91 g, 15.8 mmol, 81%). The crude product was pure enough to perform the next step. The $LiAlH_4$ (0.93 g, 24.5 mmol) was dissolved in 15 mL dry THF, stirred for 5 min under inert atmosphere. Trans-3-undecenoic acid (1.5 g, 8.15 mmol) was dissolved in 5 mL THF and added slowly. The reaction was allowed to continue for 4 h under inert atmosphere, then 2 mL H_2O was added to quench the reaction, and 1 M HCl was added until pH < 3. Most of the THF was removed *in vacuo*, and the residue was diluted with 10 mL H_2O, and extracted with CH_2Cl_2 (3 × 30 mL). The combined organic layers were dried with Na_2SO_4, and the solvent was removed *in vacuo*. The resulting residue was purified by column chromatography over silica (hexane, 30% ethyl acetate) to give pure trans-3-undecen-1-ol **4f** (1.3 g, 7.7 mmol, 94%). The trans-3-dodecen-1-ol **4g** was also synthesized following the same method as for **4f** and had comparable yield.

Trans-3-undecen-1-ol (4f)

^{1}H NMR (400 MHz, $CDCl_3$): 0.88 (t, 3H, $J = 6.8$ Hz), 1.27–1.39 (m, 10H), 2.01 (q, 2H, $J = 6.4$ Hz), 2.26 (q, 2H, $J = 6.4$ Hz), 3.61 (t, 2H, $J = 6.4$ Hz), 5.37 (dt, 1H, $J = 15.2$, 7.2 Hz), 5.55 (dt, 1H, $J = 15.2$, 6.8 Hz); ^{13}C NMR (100 MHz, $CDCl_3$): 14.2, 22.8, 29.3, 29.4, 29.6, 32.0, 32.8, 36.1, 62.2, 125.8, 134.4.

Trans-3-dodecen-1-ol (4g)

^{1}H NMR (400 MHz, $CDCl_3$): 0.88 (t, 3H, $J = 7.2$ Hz), 1.22–1.37 (m, 12 H), 2.01 (q, 2H, $J = 6.4$ Hz), 2.26 (q, 2H, $J = 6.4$ Hz), 3.62 (t, 2H, $J = 6.4$ Hz), 5.37 (dt, 1H, $J = 15.2$, 7.2 Hz), 5.56 (dt, 1H, $J = 15.2$, 6.8 Hz);

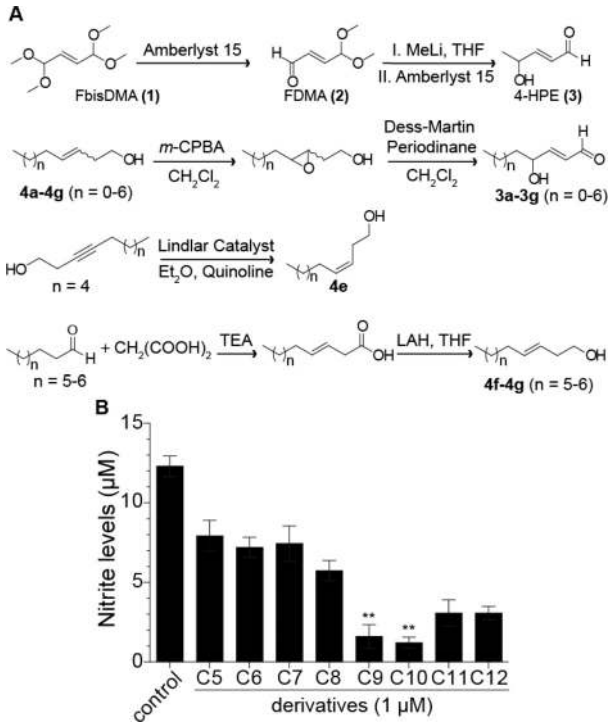

Fig. 2. Synthesis and activity of **C5–C12** 4-hydroxy-2-*(E)*-alkenal derivatives. (A) Synthesis of 4-hydroxy-2-*(E)*-alkenal derivatives **C5–C12**. 4-HPE [3] is described as **C5** in the text and compounds **3a–3g** represents **C6** to **C12** where $n = 0$–6 correspondingly. (B) Nitrite levels from LPS-activated macrophage treated with 1 μM 4-hydroxy-2-*(E)*-alkenal derivatives **C5–C12**for 24 h. Experiments were performed at least 3 times and error bars represent standard error of mean. $^{**}P < 0.01$.

^{13}C NMR (100 MHz, $CDCl_3$): 14.3, 22.8, 29.4, 29.5, 29.7, 29.7, 32.1, 32.8, 36.1, 62.2, 125.8, 134.6.

Cell culture

RAW 264.7 cells were cultured in DMEM media supplemented with 10% FBS and 1% penicillin/streptomycin and kept in culture at 37 °C in a 5% CO_2 environment. Cells were kept in culture for no longer than a month and routinely checked for LPS responsiveness every two to three passages via detection of nitrite production measured using the Griess assay.

Cell viability measurement

Remaining cells from the Griess assay were used for viability measurement using the MTT Cell Proliferation assay kit from ATCC following manufacturer's instruction. Absorbance was read at 550 nm using the Sunrise™ plate reader by TECAN. Percent viability of treated cells was calculated relative to the LPS-activated treated with DMSO control as 100% viability.

Nitrite level measurement

RAW 264.7 cells were plated at 1×10^6 cells/well in a 96-well plate and allowed to attach for 3 h before simultaneous activation with 10 ng/mL LPS and treated with 4-hydroxy-2-(*E*)-alkenal derivatives (**C5–C12**, **C9** being 4-HNE) or 0.25% DMSO control. 4-Hydroxy-2-(*E*)-alkenal derivatives were freshly made in DMSO. LPS-activated cells were treated with varying concentrations of 4-HNE for either 30 min or 24 h. For studies of other 4-hydroxy-2-(*E*)-alkenal derivatives, LPS-activated cells were treated with 1 μM derivatives for 24 h. Nitrite levels were measured via Griess assay according to manufacturer's specifications using 100 μL Griess reagent with 100 μL sample supernatant. Absorbance was read at 550 nm using the Sunrise™ plate reader by TECAN (Mannedorf, Switzerland).

Immunoblot analysis

RAW 264.7 cells were plated at 4×10^6 cells/60 mm plate and allowed to attach for 3 h. Cells were activated with 10 ng/mL LPS and treated with varying concentrations of 4-HNE, DMSO control, or LPS with DMSO control and harvested for immunoblot analysis and quantitative RT-PCR. Proteins were isolated via lysing the cells with RIPA Buffer containing protease inhibitors and equal amounts of proteins were loaded into a Novex 4–20% Tris–Glycine gel. Proteins were transferred to a PVDF membrane, blocked with 5% non-fat dry skim milk in 0.5% Tris-buffered saline containing Tween-20 (TBST), and probed with antibodies. Primary antibodies were diluted 1:500 to 1:1000 and secondary horse-radish peroxidase antibodies were diluted 1:5000. Antibodies were detected using ECL plus with autoradiography.

Quantitative RT-PCR

Cells harvested for the immunoblot analysis were also harvested for quantitative RT-PCR. Total RNA was extracted using the PureLink™ RNA Mini Kit followed by reverse transcription reaction using the Superscript® III Reverse Transcriptase. PCR was performed using TaqMan® Gene Expression Assay iNOS, HO-1, NQO1 and GCLC probes (Assay ID: Mm01309902_m1, Mm00516007_m1, Mm00500821_m1, Mm00802655_m1, respectively), PrimeTime qPCR assay (Assay ID: Mm.PT.42.122532.g) 18s rRNA control probe with TaqMan® Fast Universal PCR Master Mix. Amplification was performed using the 7500 Fast Real-Time PCR system (95 °C for 20 s, followed by 40 cycles of 95 °C for 3 s, and 60 °C for 30 s) and the 7500 Fast System SDS Software-Sequence Detection Software version 1.3.1.21 by Applied Biosystems.

iNOS activity assay

iNOS activity was measured using the iNOS activity kit via detection of radiolabeled arginine (arginine monohydrochloride L-[2,3,4-^{3}H]) conversion to L-citrulline. Reactions were prepared according to manufacturer's instructions using the iNOS (murine recombinant) enzyme. Each reaction was treated with various 4-HNE concentrations and allowed to proceed at room temperature for 1 h. Radioactivity was quantified by counts per minute (CPM) with 1450 MicroBeta TriLux Microplate Scintillation Counter. The positive control contained iNOS enzyme, and the negative control contained the iNOS enzyme treated with a NOS competitive inhibitor L-N^G-nitroarginine (L-NNA).

Bone marrow derived macrophage isolation and treatment

Bone marrow derived macrophages (BMDM) from 6–8 week old C57BL/J6 mice (wild-type) and Nrf2 knockout mice ($Nrf2^{-/-}$) were isolated and plated in DMEM medium supplemented with 10% FBS, 1% penicillin/streptomycin and M-CSF. Fresh medium containing M-CSF was added after 3 days of incubation. Cells were washed with PBS 2–3 times to remove non-macrophage cells and a non-enzymatic detaching solution was used to collect BMDM. Cells were plated at 4×10^6 cells/60 mm plate in DMEM medium supplemented with 10% FBS and 1% penicillin/streptomycin, and cultured overnight. BMDM were activated with 500 ng/mL LPS and treated with varying concentrations of 4-HNE or 0.05% DMSO control. Cells were harvested for Griess assay and MTT analysis after a 48 h treatment. All experiments performed were in accordance with an approved protocol by the Institutional Animal Care and Use Committee at Case Western Reserve University.

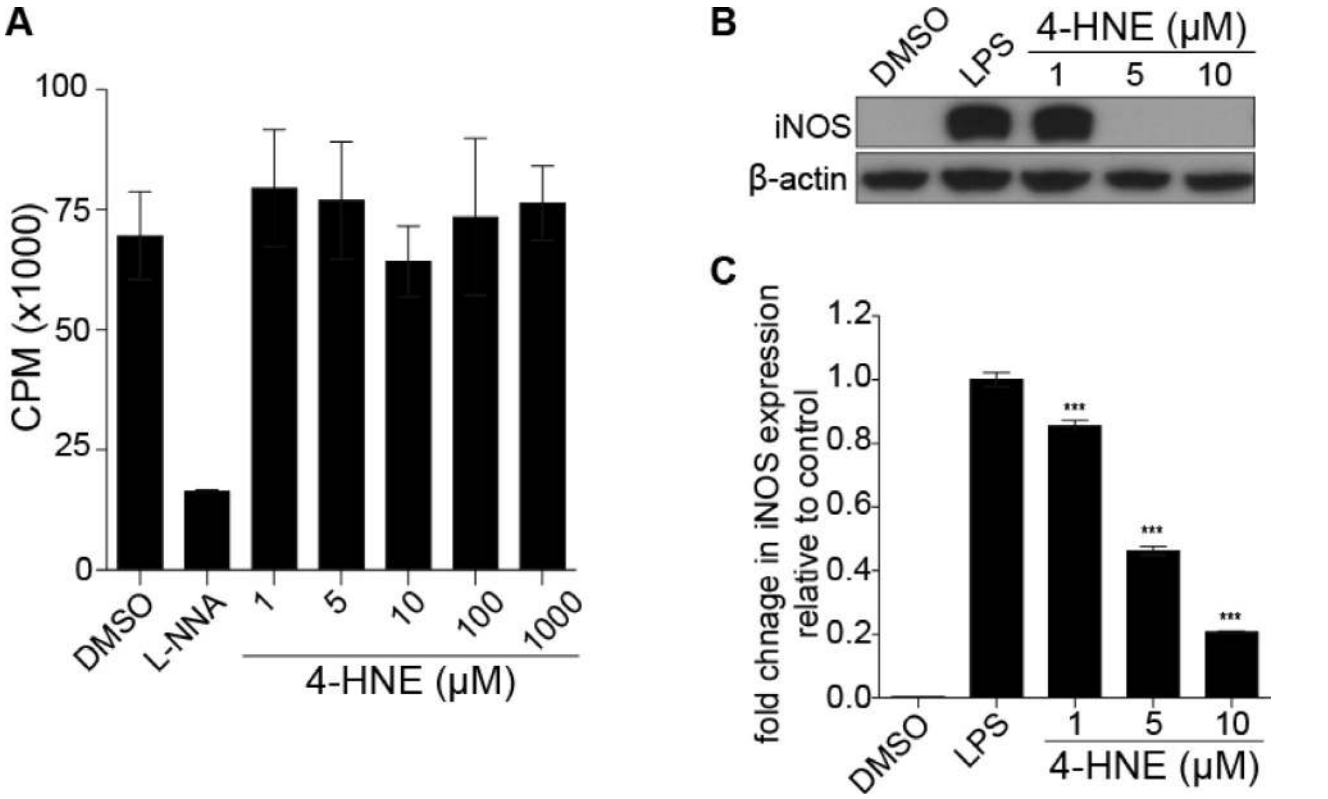

Fig. 3. (A) iNOS activity was measured via quantification of radiolabeled L-arginine to L-citrulline conversion. iNOS enzyme alone served as positive control while iNOS enzyme treated with N^{ω}-nitro-L-arginine (L-NNA) inhibitor served as negative control. (B) Immunoblot analysis of iNOS protein levels in 4-HNE treated LPS-activated macrophage treated for 18 h. DMSO treated cells were used as negative control while DMSO treated LPS-activated cells were used as positive control. β-actin was used as protein loading control. (C) mRNA levels of 4-HNE treated LPS-activated macrophage treated for 18 h. Fold change in expression were calculated relative to DMSO treated LPS-activated iNOS expression which was normalized to 18s rRNA expression. Experiments were performed at least 3 times and error bars represent standard error of mean. $^{***}P < 0.001$.

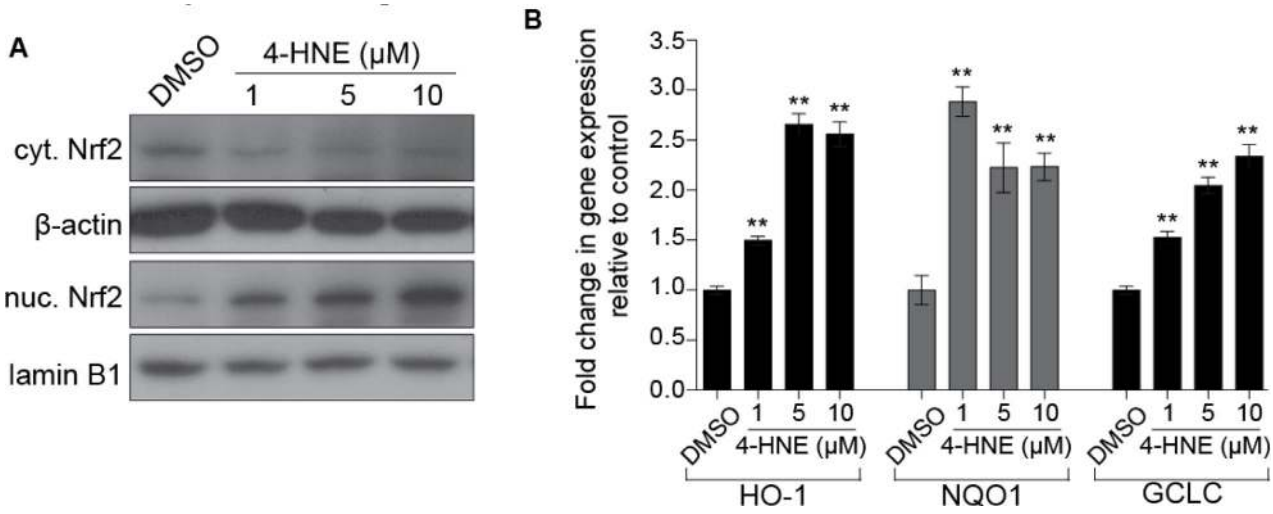

Fig. 4. (A) Immunoblot analysis of Nrf2 protein levels in the cytoplasm and nucleus. RAW 264.7 cells were treated with increasing concentrations of 4-HNE for 5 min. β-actin and lamin B1 were used as loading controls. (B) mRNA levels of 4-HNE treated macrophage were treated for 4 h. Fold change in expression was calculated relative to DMSO treated HO-1, NQO1, and GCLC expression which was normalized to 18s rRNA expression. Experiments were performed at least 3 times and error bars represent standard error of mean. $^{**}P < 0.01$.

Conjugated 4-HNE-GSH LC-MS measurement

4-hydroxydecanenal-GSH, and 4-HNE-GSH Michael addition adducts were assayed from our previously published methods, with modification [1,22,33,43]. Briefly, media (1 mL) or cell lysates (32.5 μL) from 4-HNE treated RAW 264.7 cells for 15 min or 18 h were spiked with 0.25 nmol of 4-hydroxydecanenal-GSH (internal standard). Media from culture and cell lysates were treated with 4 or 0.2 mL acetonitrile, respectively, to precipitate proteins. After centrifugation at 4 °C, the supernatant was dried under N_2 gas. The dried residue was dissolved in 100 μL Milli-Q water, 40 μL was injected for LC-MS analysis. The LC-MS was acquired in a Dionex-UltiMate 3000 HPLC using Thermo Scientific Hypersil GOLD C18 column (150 × 2.1 mm^2) with a guard column (Hypersil GOLD C18 5 μm,

10 × 2.1 mm^2) combined with a 4000 Qtrap mass spectrometer (Applied Biosystems, Foster City, CA). The chromatographic method was developed at 0.2 mL/min (i) from 0 to 25 min with a 1–45% gradient of buffer B (95% acetonitrile, 5% water, and 0.25% formic acid) in buffer A (95% water, 5% acetonitrile, and 0.25% formic acid), (ii) from 25 to 26 min with a 45–90% gradient of buffer B in buffer A, (iii) from 26 to 31 min with 90% buffer B in buffer A, and (iv) from 31 to 32 min with a decreasing 90–1% gradient of buffer B in buffer A, with 10 min of equilibration with 99% buffer A before the next injection. The 4000 QTrap mass spectrometer was operated under positive ionization mode with the following source settings: turbo-ion-spray source at 600 °C, N_2 nebulization at 65 psi, N_2 heater gas at 55 psi, curtain gas at 30 psi, collision-activated dissociation gas pressure held at high, turbo-ion-spray voltage at 5500 V, declustering potential at 90 V, entrance potential at 10 V, collision energy at 50 V, and collision cell exit potential at 10 V. Data acquisition was performed in multiple reaction monitoring mode monitoring the transition of $[M + H] + m/z$ 464 in Q1 to [MH−156] + m/z 308 (protonated GSH) in Q3 as quantifier. The internal standard precursor ion and product ion were at m/z 475 and 308, respectively.

Results and discussion

Identification of a negative feedback loop for 4-HNE production.

Our initial experiment examined whether 4-HNE could modulate inducible NO formation in RAW 264.7 (RAW) culture macrophages stimulated with lipopolysaccharide (LPS). Using the standard Griess assay, we measured NO production after a 24 h exposure to LPS and various concentrations of 4-HNE to examine steady state levels of NO production (Fig. 1A, Supplementary Figs. S1 and S2). Surprisingly, we observed a dramatic decrease in NO production at 4-HNE concentrations greater than 1 μM (Fig. 1A). The observed decrease in NO production is not gradual as demonstrated by the abrupt decrease of NO levels over concentration ranges as small as 2.5-fold. Further, the observed effect cannot be attributed to toxicity (Supplementary Fig. S3). This result is physiologically relevant given that the basal concentrations of 4-HNE found ubiquitously throughout mammalian tissues range from 100 nM to 1 μM [13,25]. The biological significance of this finding becomes evident when considering the origins of LPO products. The initial hydrogen abstraction step in LPO is ascribed to the chemical reactivity of oxidants such as superoxide and NO. Because 4-HNE is inhibiting the formation of NO, it is effectively inhibiting its own production by limiting the production of NO which is ultimately converted to the family of oxidants responsible for non-enzymatic lipid peroxidation and consequently the production of 4-HNE. We hypothesized that these observations represent the discovery of a negative feedback loop for the production of 4-HNE through inhibition of oxidant formation.

To examine whether 4-HNE has an effect on the constitutively expressed isoform (endothelial eNOS) in RAW 264.7 cells [40], we tested the effects of 4-HNE at various concentrations at earlier time-points before iNOS expression could occur [9]. After 30 min of exposure to 4-HNE, no effect was observed in the nM to μM range, however at higher concentrations (9–10 mM, Fig. 1B) a dramatic increase in NO production was observed, with nitrite concentrations reaching greater than 20 μM. Since it takes at least 8 h to induce NO production (Supplementary Fig. S1), the increase in NO observed at 30 min cannot be attributed to stimulation via LPS. It is unclear whether this effect is due to a specific activation of eNOS [41], or a secondary effect that is related to the toxicity inherent in these high concentrations of 4-HNE [24]. Additional studies are required to further determine the mechanism for the observed spike in NO levels during the first 30 min in 4-HNE-treated RAW cells. Regardless, given our laboratory's interests in iNOS, we decided to further explore the mechanistic underpinnings of the observed negative feedback profile.

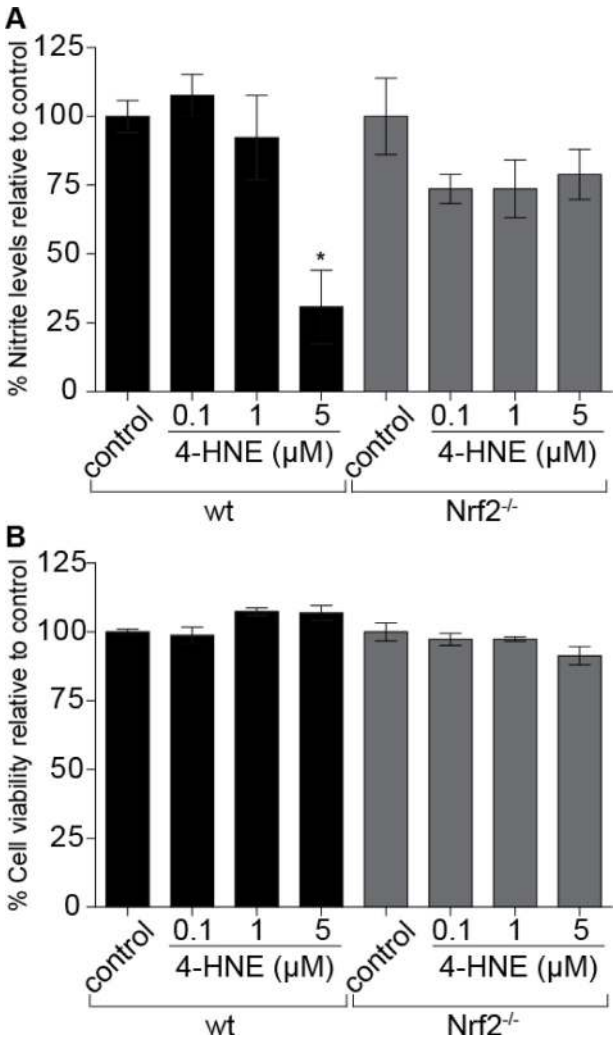

Fig. 5. Nitrite levels and viability in 4-HNE treated activated primary macrophage cells. (A) Nitrite levels were measured via Griess assay in cells simultaneously activated with 500 ng/mL LPS and treated with varying concentrations of 4-HNE for 48 h (B) cell viability was measured using MTT assay. LPS-activated cells treated with DMSO were used as control. Experiments were performed at least 3 times and error bars represent standard error of mean. $^*P < 0.01$.

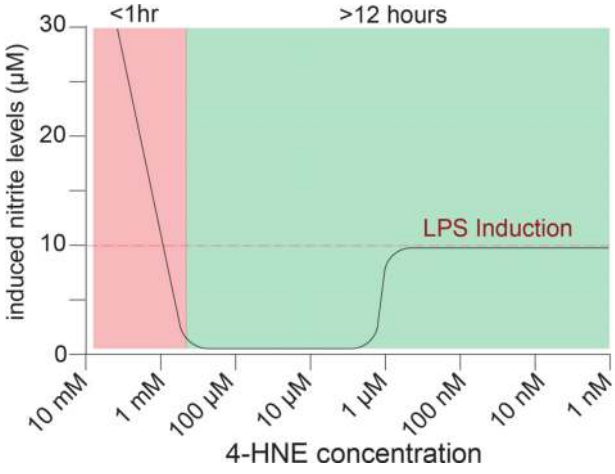

Fig. 6. A model for 4-HNE control of induced nitric oxide production. At low 4-HNE concentrations over long time periods, there is an Nrf2-dependent negative feedback loop that inhibits LPS-induced nitric oxide production with an inflection at approximately 1 μM (green region). At higher concentrations a positive feedback loop is present whereby increasing concentrations of 4-HNE in turn elicits higher concentrations of nitric oxide during a short time period (red region).

Specificity of 4-hydroxy-2-(E)-alkenal C9–C10 derivatives on NO inhibition.

Our next experiment aimed to test whether the observed phenotype was specific for 4-HNE, or simply a non-specific effect derived from the electrophilic nature of the molecule. To test this, several 4-hydroxy-2-(*E*)-alkenal derivatives with varied chain lengths (**C5–C12**) were synthesized and evaluated for inhibition of NO production as above. 4-Hydroxy-2-(*E*)-pentenal (**C5**) was synthesized via a minor modification of the reported procedure (Fig. 2A) [36]. The other 4-hydroxy-2-(*E*)-alkenal derivatives (**C6–C12**) were synthesized using a new strategy inspired by Gardner et al. [15], which treats homoallylic alcohols of appropriate chain length with *m*-CPBA to afford the 3,4-epoxyalcohols that are then oxidized with Dess–Martin periodinane. The resulting 3,4-epoxyaldehydes undergo an in situ α-hydrogen elimination and concomitant epoxide opening forming of the desired 4-hydroxy-2-(*E*)-alkenals.

Evaluation of NO production in activated macrophages displayed a clear pattern whereby the **C9** (4-HNE) and **C10** alkenals showed the most pronounced decrease in NO production (Fig. 2B). This result was not due to toxicity (Supplementary Fig. S4), and points to the observed negative feedback being selective for 4-HNE. The observation that **C10** is slightly more potent is clear and repeatable across multiple concentrations. On this point, in our recent findings, we have found the presence of glutathionylated **C10** in rat liver and heart tissues, and others have reported the presence of **C10** in tissues [18]. It is plausible that the similar molecular volume of **C9** and **C10** effectively renders them identical in their effective modulation of signal transduction pathways controlling macrophages for NO production *in vivo*.

Mechanism of inhibition by 4-HNE of NO production

From a mechanistic point of view, we proposed two possible explanations for the observed phenotypes. The first was that 4-HNE inhibited the enzymatic activity of iNOS, resulting in decreased NO production; the second explanation is rationalized as a consequence of decreased iNOS expression. To differentiate between these two possibilities we first investigated the effect of varying 4-HNE concentrations on recombinant murine iNOS. Activity was measured from the conversion of radiolabeled L-arginine to L-citrulline using a standard assay and quantified using scintillation counts per minute (CPM) [4]. We tested the activity of recombinant iNOS at various 4-HNE concentrations, which correlated to the inhibitory concentrations observed in Fig. 2A. Between 1 μM and 1 mM no appreciable perturbation to iNOS activity was seen (Fig. 3A).

From these data, we concluded that 4-HNE is not a direct enzymatic inhibitor of iNOS. To explore our alternate hypothesis, we examined iNOS expression utilizing immunoblot and quantitative RT-PCR analysis of 4-HNE treated LPS-activated RAW macrophages. We observed that iNOS protein levels were not detectable in cells treated with 5 μM and above 4-HNE (Fig. 3B). This observation positively correlated with quantitative RT-PCR analysis (Fig. 3C) that showed a dose dependent inhibition in iNOS transcript by 4-HNE. Taken together, it is clear that the observed inhibition of oxidant formation is due to an inhibition of expression of iNOS. This observation is consistent with previous reported in other cell lines [17,39].

Activation of Nrf2 signaling by 4-HNE suppresses NO production.

Previous reports have demonstrated that molecules which activate Nrf2 transcription also perturb iNOS expression [23]. Based on these observations, we explored the hypothesis that 4-HNE inhibits iNOS expression through the activation of Nrf2. Canonical activation of Nrf2 typically involves a small molecule activator that will specifically interact with the repressor protein, Keap1. When this occurs, Nrf2 dissociates from Keap1, translocates to the nucleus and effects the transcription of genes containing an antioxidant response element (ARE). To test whether 4-HNE affects nuclear translocation of Nrf2, we performed immunoblot analysis of cytoplasmic and nuclear Nrf2 protein in RAW macrophages treated with 4-HNE concentrations ranging from 1 to 10 μM. As seen in Fig. 4A, cytoplasmic Nrf2 protein levels decreased in the presence of 1 μM 4-HNE, while nuclear Nrf2 protein levels increased in a dose-dependent manner after treatment for 5 min.

To further demonstrate Nrf2 activation by 4-HNE in RAW macrophages, we performed a series of quantitative RT-PCR analyses of the Nrf2 target genes: heme oxygenase (HO-1), NAD(P)H:quinone (NQO1) and γ-glutamylcysteine synthetase (GCLC). Fig. 4B, clearly shows marked increases in transcription for all three, with HO-1 and GCLC increasing 1.5-fold, while NQO1 gene expression increased 3-fold. At concentrations of 5 μM and above, HO-1, NQO1 and GCLC gene expression increased 2- to 3-fold relative to control. Previous studies have shown that 4-HNE induces Nrf2 translocation [44,45], but Nrf2 mediated iNOS suppression and subsequent inhibition of NO production by 4-HNE has not been addressed. Taken together, these results clearly implicate activation of Nrf2 transcription as a probable mechanism to explain the observed changes in iNOS expression.

To confirm our proposed mechanism, we initiated a series of experiments using primary macrophages derived from either wild-type (wt), or Nrf2 deficient mice ($Nrf2^{-/-}$). We isolated bone marrow derived macrophages (BMDMs) from wt and $Nrf2^{-/-}$ mice and activated the cells with LPS. Activated BMDM were treated with 0.1–5 μM 4-HNE for 48 h. In the presence of 5 μM 4-HNE, we observed the same decrease in NO as in the RAW macrophages, albeit with a slightly attenuated response (Fig. 5A). This decrease in NO was not due to toxicity (Fig. 5B). However, in $Nrf2^{-/-}$ BMDMs, no appreciable differences were observed for NO production. Given the above experiment, we can ascribe the observed ability of 4-HNE to suppress iNOS and inhibit NO formation to be a direct result of Nrf2 activation. This is further supported by a study demonstrating 4-HNE directly adducting to transcriptional inhibitor Keap1 [26].

Here, we have demonstrated that 4-HNE modulates the production of the biological oxidant NO, which can further react with other species, such as superoxide, to form the powerful oxidants responsible for lipid peroxidation. Further, we had provided evidence that this effect is a result of the activation of the Nrf2 transcription factor. We would postulate that this activation is as a result of 4-HNE directly adducting one of the surface cysteine residues of the repressor protein, Keap1, which has been previously shown by others in other systems [21,26]. We carefully considered alternate hypotheses including whether the observed effects could have arisen downstream of another process or as a result of a 4-HNE metabolite. To this end, we evaluated the state of reduced intracellular glutathione, and observed no appreciable difference (Supplementary Fig. S5) [6]. Further, based on our own work investigating the metabolic fate of 4-HNE we concluded that it is highly probable that the active intracellular molecule is 4-HNE [33,43].

The significance of these observations is rooted in chemical processes that lead to the formation of LPO products. As mentioned earlier, the first step in this process is radical hydrogen abstraction of PUFA by reactive oxygen and reactive nitrogen substances (ROS and RNS, respectively), leading to the production of NO directly and the formation of 4-HNE in the presence of PUFAs. The finding that 4-HNE, in turn, regulates the production of NO has the hallmark of a negative feedback pathway. We propose that these findings argue for an evolved feedback pathway to control the concentration of 4-HNE (and other LPO products) in tissues that express inflammatory mediators (such as iNOS) indirectly via the production of ROS and RNS.

Conclusion

The fact that the observed inhibitory concentrations of 4-HNE correspond to the observed physiologic concentrations lends further credence to our hypothesis that 4-HNE is an essential endogenous regulator of NO production mediated through Nrf2 activation. The significance of our study is that we demonstrated the involvement of Nrf2 in suppressing NO production in 4-HNE treated cells. Taken together we have devised a model of the expression control of 4-HNE as shown in Fig. 6 that would argue for the production of 4-HNE as a carefully regulated process with an observed negative feedback loop. High concentrations of 4-HNE have been observed during oxidative stress and in many disease states (red region). However, at low concentrations over long time periods, there is an Nrf2-dependent negative feedback loop that inhibits LPS-induced nitric oxide production with an inflection at approximately 1 μM (green region) that is dependent on Nrf2. This model stands in contrast to views in the field that see 4-HNE as a cytotoxic xenobiotic causative of multiple disease states.

Acknowledgements

The work was supported by grants from the NIH, R01CA157735 and R03CA132168, and Reuter Foundation to G.P.T. and J. J.T., Landon Foundation INNOVATOR award from AACR and NSF CAREERMCB-0844801 to G.P.T., and an NIH fellowship, F31CA134211 to T.N.G.

Appendix A. Supplemental Materials

Supplementary material associated with this article can be found, in the online version, at http://dx.doi.org/10.1016/j.redox.2014.04.009

References

[1] J. Alary, Y. Fernandez, L. Debrauwer, E. Perdu, F. Gueraud, Identification of intermediate pathways of 4-hydroxynonenal metabolism in the rat, Chemical Research in Toxicology 16 (2003) 320–327. http://dx.doi.org/10.1021/tx025671k, 12641432.

[2] Y. Ando, T. Brannstrom, K. Uchida, N. Nyhlin, B. Nasman, O. Suhr, et al, Histochemical detection of 4-hydroxynonenal protein in Alzheimer amyloid, Journal of the Neurological Sciences 156 (1998) 172–176. http://dx.doi.org/10.1016/S0022-510X(98)00042-2, 9588853.

[3] V.N. Bochkov, O.V. Oskolkova, K.G. Birukov, A.L. Levonen, C.J. Binder, J. Stockl, Generation and biological activities of oxidized phospholipids, Antioxidants and Redox Signaling 12 (2010) 1009–1059. http://dx.doi.org/10.1089/ars.2009.2597, 19686040.

[4] D.S. Bredt, S.H. Snyder, Nitric oxide:a physiologic messenger molecule, Annual Review of Biochemistry 63 (1994) 175–195. http://dx.doi.org/10.1146/annurev.bi.63.070194.001135, 7526779.

[5] M.S. Brown, J.L. Goldstein, Lipoprotein metabolism in the macrophage: implications for cholesterol deposition in atherosclerosis, Annual Review of Biochemistry 52 (1983) 223–261. http://dx.doi.org/10.1146/annurev.bi.52.070183.001255, 6311077.

[6] Y. Buchmuller-Rouiller, S.B. Corrandin, J. Smith, P. Schneider, A. Ransijn, C.V. Jongeneel, et al, Role of glutathione in macrophage activation: effect of cellular glutathione depletion on nitrite production and leishmanicidal activity, Cellular Immunology 164 (1995) 73–80. http://dx.doi.org/10.1006/cimm.1995.1144, 7543373.

[7] N.Y. Calingasan, K. Uchida, G.E. Gibson, Protein-bound acrolein:a novel marker of oxidative stress in Alzheimer's disease, Journal of Neurochemistry 72 (1999) 751–756. http://dx.doi.org/10.1046/j.1471-4159.1999.0720751.x, 9930749.

[8] Z.H. Chen, Y. Saito, Y. Yoshida, A. Sekine, N. Noguchi, E. Niki, 4-Hydroxynonenal induces adaptive response and enhances PC12 cell tolerance primarily through induction of thioredoxin reductase 1 via activation of Nrf2, Journal of Biological Chemistry 280 (2005) 41921–41927, 16219762.

[9] L. Connelly, M. Palacios-Callender, C. Ameixa, S. Moncada, A.J. Hobbs, Biphasic regulation of NF-kappa B activity underlies the pro- and anti-inflammatory actions of nitric oxide, Journal of Immunology 166 (2001) 3873–3881. http://dx.doi.org/10.4049/jimmunol.166.6.3873, 11238631.

[10] C.M. Cox, D.A. Whiting, Synthetic studies on electron transport inhibitors. Part 2. Approaches to the synthesis of myxalamide D, Journal of the Chemical Society, Perkin Transactions 1 8 (1991) 1907–1911. http://dx.doi.org/10.1039/P19910001907.

[11] S.S. Davies, L. Guo, Lipid peroxidation generates biologically active phospholipids including oxidatively N-modified phospholipids, Chemistry and Physics of Lipids 181 (2014) 1–33, 24704586.

[12] A.T. Dinkova-Kostova, K.T. Liby, K.K. Stephenson, W.D. Holtzclaw, X. Gao, N. Suh, et al, Extremely potent triterpenoid inducers of the phase 2 response: correlations of protection against oxidant and inflammatory stress, Proceedings of the National Academy of Sciences of the United States of America 102 (2005) 4584–4589. http://dx.doi.org/10.1073/pnas.0500815102, 15767573.

[13] H. Esterbauer, R.J. Schaur, H. Zollner, Chemistry and biochemistry of 4-hydroxynonenal, malonaldehyde and related aldehydes, Free Radical Biology and Medicine 11 (1991) 81–128. http://dx.doi.org/10.1016/0891-5849(91)90192-6, 1937131.

[14] H.J. Forman, D.A. Dickinson, Introduction to serial reviews on 4-hydroxy-2-nonenal as a signaling molecule, Free Radical Biology and Medicine 37 (2004) 594–596. http://dx.doi.org/10.1016/j.freeradbiomed.2004.06.009, 15288117.

[15] H. Gardner, R. Bartelt, D. Weisleder, A facile synthesis of 4-hydroxy-2(E)-nonenal, Lipids 27 (1992) 686–689. http://dx.doi.org/10.1007/BF02536025.

[16] T.N. Gatbonton-Schwager, J.J. Letterio, G.P. Tochtrop, Bryonolic acid transcriptional control of anti-inflammatory and antioxidant genes in macrophages in vitro and in vivo, Journal of Natural Products 75 (2012) 591–598. http://dx.doi.org/10.1021/np200823p, 22339499.

[17] Y. Hattori, S. Hattori, K. Kasai, 4-hydroxynonenal prevents NO production in vascular smooth muscle cells by inhibiting nuclear factor-kappaB-dependent transcriptional activation of inducible NO synthase, Arteriosclerosis, Thrombosis, and Vascular Biology 21 (2001) 1179–1183. http://dx.doi.org/10.1161/hq0701.092135, 11451748.

[18] I. Hubatsch, M. Ridderstrom, B. Mannervik, Human glutathione transferase A4-4: an Alpha class enzyme with high catalytic efficiency in the conjugation of 4-hydroxynonenal and other genotoxic products of lipid peroxidation, Biochemical Journal 330 (1998) 175–179, 9461507.

[19] T. Ishii, K. Itoh, E. Ruiz, D.S. Leake, H. Unoki, M. Yamamoto, et al, Role of Nrf2 in the regulation of CD36 and stress protein expression in murine macrophages: activation by oxidatively modified LDL and 4-hydroxynonenal, Circulation Research 94 (2004) 609–616. http://dx.doi.org/10.1161/01.RES.0000119171.44657.45, 14752028.

[20] W.E.M. Lands, The biosynthesis and metabolism of prostaglandins, Annual Review of Physiology 41 (1979) 633–652. http://dx.doi.org/10.1146/annurev.ph.41.030179.003221, 219768.

[21] A.L. Levonen, A. Landar, A. Ramachandran, E.K. Ceaser, D.A. Dickinson, G. Zanoni, et al, Cellular mechanisms of redox cell signalling: role of cysteine modification in controlling antioxidant defences in response to electrophilic lipid oxidation products, Biochemical Journal 378 (2004) 373–382. http://dx.doi.org/10.1042/BJ20031049, 14616092.

[22] Q. Li, K. Tomcik, S. Zhang, M.A. Puchowicz, G.F. Zhang, Dietary regulation of catabolic disposal of 4-hydroxynonenal analogs in rat liver, Free Radical Biology and Medicine 52 (2012) 1043–1053, 22245097.

[23] H. Liu, A.T. Dinkova-Kostova, P. Talalay, Coordinate regulation of enzyme markers for inflammation and for protection against oxidants and electrophiles, Proceedings of the National Academy of Sciences of the United States of America 105 (2008) 15926–15931. http://dx.doi.org/10.1073/pnas.0808346105, 18838692.

[24] Y. Maejima, S. Adachi, H. Ito, K. Nobori, M. Tamamori-Adachi, M. Isobe, Nitric oxide inhibits ischemia/reperfusion-induced myocardial apoptosis by modulating cyclin A-associated kinase activity, Cardiovascular Research 59 (2003) 308–320. http://dx.doi.org/10.1016/S0008-6363(03)00425-5, 12909314.

[25] U.M. Marinari, M. Nitti, M.A. Pronzato, C. Domenicotti, Role of PKC-dependent pathways in HNE-induced cell protein transport and secretion, Molecular Aspects of Medicine 24 (2003) 205–211. http://dx.doi.org/10.1016/S0098-2997(03)00015-3, 12892998.

[26] M. McMahon, D.J. Lamont, K.A. Beattie, J.D. Hayes, Keap1 perceives stress via three sensors for the endogenous signaling molecules nitric oxide, zinc, and alkenals, Proceedings of the National Academy of Sciences of the United States of America 107 (2010) 18838–18843. http://dx.doi.org/10.1073/pnas.1007387107, 20956331.

[27] I.G. Minko, I.D. Kozekov, T.M. Harris, C.J. Rizzo, R.S. Lloyd, M.P. Stone, Chemistry and biology of DNA containing 1,N(2)-deoxyguanosine adducts of the alpha,beta-unsaturated aldehydes acrolein, crotonaldehyde, and 4-hydroxynonenal, Chemical Research in Toxicology 22 (2009) 759–778. http://dx.doi.org/10.1021/tx9000489, 19397281.

[28] I. Nakashima, W. Liu, A.A. Akhand, K. Takeda, Y. Kawamoto, M. Kato, et al, 4-Hydroxynonenal triggers multistep signal transduction cascades for suppression of cellular functions, Molecular Aspects of Medicine 24 (2003) 231–238. http://dx.doi.org/10.1016/S0098-2997(03)00018-9, 12893001.

[29] K. Okamoto, S. Toyokuni, K. Uchida, O. Ogawa, J. Takenewa, Y. Kakehi, et al, Formation of 8-hydroxy-2′-deoxyguanosine and 4-hydroxy-2-nonenal-modified proteins in human renal-cell carcinoma, International Journal of Cancer (Journal International du Cancer) 58 (1994) 825–829, 7523311.

[30] C.W. Parker, Lipid mediators produced through the lipoxygenase pathway, Annual Review of Immunology 5 (1987) 65–84. http://dx.doi.org/10.1146/annurev.iy.05.040187.000433, 3036183.

[31] B.V.S.K. Rao, P. Vijayalakshmi, R. Subbarao, Synthesis of long-chain (E)-3-alkenoic acids by the Knoevenagel condensation of aliphatic aldehydes with malonic acid, Journal of the American Oil Chemists' Society 70 (1993) 297–299. http://dx.doi.org/10.1007/BF02545311.

[32] Y. Riahi, G. Cohen, O. Shamni, S. Sasson, Signaling and cytotoxic functions of 4-hydroxyalkenals, American Journal of Physiology – Endocrinology and Metabolism 299 (2010) E879–E886, 20858748.

[33] S. Sadhukhan, Y. Han, G.F. Zhang, H. Brunengraber, G.P. Tochtrop, Using isotopic tools to dissect and quantitate parallel metabolic pathways, Journal of the American Chemical Society 132 (2010) 6309–6311. http://dx.doi.org/10.1021/ja100399m, 20408520.
[34] C. Schneider, An update on products and mechanisms of lipid peroxidation, Molecular Nutrition and Food Research 53 (2009) 315–321. http://dx.doi.org/10.1002/mnfr.200800131, 19006094.
[35] C. Schneider, N.A. Porter, A.R. Brash, Routes to 4-hydroxynonenal: fundamental issues in the mechanisms of lipid peroxidation, Journal of Biological Chemistry 283 (2008) 15539–15543, 18285327.
[36] M. Seck, B. Seon-Meniel, J.-C. Jullian, X. Franck, R. Hocquemiller, B. Figadere, Synthesis of C1-C6 fragment of caribenolide I, Letters in Organic Chemistry 3 (2006) 390–395. http://dx.doi.org/10.2174/157017806776611818.
[37] D. Steinberg, S. Parthasarathy, T.E. Carew, J.C. Khoo, J.L. Witztum, Beyond cholesterol. Modifications of low-density lipoprotein that increase its atherogenicity, New England Journal of Medicine 320 (1989) 915–924. http://dx.doi.org/10.1056/NEJM198904063201407, 2648148.
[38] K. Uchida, 4-Hydroxy-2-nonenal:a product and mediator of oxidative stress, Progress in Lipid Research 42 (2003) 318–343. http://dx.doi.org/10.1016/S0163-7827(03)00014-6, 12689622.
[39] F. Vaillancourt, B. Morquette, Q. Shi, H. Fahmi, P. Lavigne, Battista J.A. Di, et al, Differential regulation of cyclooxygenase-2 and inducible nitric oxide synthase by 4-hydroxynonenal in human osteoarthritic chondrocytes through ATF-2/CREB-1 transactivation and concomitant inhibition of NF-kappaB signaling cascade, Journal of Cellular Biochemistry 100 (2007) 1217–1231. http://dx.doi.org/10.1002/jcb.21110, 17031850.
[40] B. Wegiel, D. Gallo, E. Csizmadia, T. Roger, E. Kaczmarek, C. Harris, et al, Biliverdin inhibits Toll-like receptor-4 (TLR4) expression through nitric oxide-dependent nuclear translocation of biliverdin reductase, Proceedings of the National Academy of Sciences of the United States of America 108 (2011) 18849–18854. http://dx.doi.org/10.1073/pnas.1108571108, 22042868.
[41] J. Whitsett, M.J. Picklo Sr., J. Vasquez-Vivar, 4-Hydroxy-2-nonenal increases superoxide anion radical in endothelial cells via stimulated GTP cyclohydrolase proteasomal degradation, Arteriosclerosis, Thrombosis, and Vascular Biology 27 (2007) 2340–2347. http://dx.doi.org/10.1161/ATVBAHA.107.153742, 17872449.
[42] J.L. Witztum, D. Steinberg, Role of oxidized low density lipoprotein in atherogenesis, Journal of Clinical Investigation 88 (1991) 1785–1792. http://dx.doi.org/10.1172/JCI115499, 1752940.
[43] G.F. Zhang, R.S. Kombu, T. Kasumov, Y. Han, S. Sadhukhan, J. Zhang, et al, Catabolism of 4-hydroxyacids and 4-hydroxynonenal via 4-hydroxy-4-phosphoacyl-CoAs, Journal of Biological Chemistry 284 (2009) 33521–33534, 19759021.
[44] Y. Zhang, M. Sano, K. Shinmura, K. Tamaki, Y. Katsumata, T. Matsuhashi, et al, 4-hydroxy-2-nonenal protects against cardiac ischemia-reperfusion injury via the Nrf2-dependent pathway, Journal of Molecular and Cellular Cardiology 49 (2010) 576–586. http://dx.doi.org/10.1016/j.yjmcc.2010.05.011, 20685357.
[45] R. Zheng, D.E. Heck, V. Mishin, A.T. Black, M.P. Shakarjian, A.N. Kong, et al, Modulation of keratinocyte expression of antioxidants by 4-hydroxynonenal, a lipid peroxidation end product, Toxicology and Applied Pharmacology 275 (2014) 113–121. http://dx.doi.org/10.1016/j.taap.2014.01.001, 24423726.